TELECOMMUNICATIONS AND RADIO ENGINEERING

VOLUME 79, ISSUE 19, 2020

begell
New York • Connecticut

TELECOMMUNICATIONS AND RADIO ENGINEERING

Volume 79, Issue 19 **2020**

CONTENTS

MICROWAVE ELECTROMAGNETICS

Compact Ku-Band Iris Polarizers for Satellite Telecommunication Systems **1673**
S.I. Piltyay, O.Yu. Sushko, A.V. Bulashenko, & I.V. Demchenko

SIGNAL PROCESSING

Neural Network Based Detection of Heterogeneities in Noisy Images **1691**
S. Abramov, A. Naumenko, V. Lukin, S. Krivenko, & I. Kaluzhinov

ANTENNAS

Design of a Dual-Band Patch Antenna using Characteristic Mode Analysis for Bluetooth and WiMax Applications **1707**
K.J. Babu, S.R. Kalva, L.V.S.T. Kammili, & S.R. Pasumarthi

Design of CPW fed UWB Antenna with Dual Notch Band using T-Shape Stub **1713**
T. Mandal, P. Mondal, & S. Das

An Investigation and Implementation of Wide Band Dielectric Resonator Antenna for 5G Wireless Communications **1725**
Ch. Raghavendra & M. Neelaveni Ammal

APPLIED RADIO PHYSICS

Development of Information Devices for Control of Objects with a Discrete Mode of Motion on the Basis of Magnetometric Converters **1735**
M.F. Smyrnyi, V.Ye. Pliuhin, A.P. Polivianchuk, & A.M. Gokov

Partial Discharge Classification using SWT and Multiscale Permutation Entropy **1747**
L. Sun & J. Song

Research on Auxiliary Diagnosis of Power Communication Field Operation and Maintenance based on CBR **1761**
Xi. Lin, W. Zhang, H. Qiu, & B. Peng

Telecommunications and Radio Engineering, 79(19):1735-1746 (2020)

APPLIED RADIO PHYSICS

DEVELOPMENT OF INFORMATION DEVICES FOR CONTROL OF OBJECTS WITH A DISCRETE MODE OF MOTION ON THE BASIS OF MAGNETOMETRIC CONVERTERS

M.F. Smyrnyi,[1] V.Ye. Pliuhin,[1] A.P. Polivianchuk,[1] & A.M. Gokov[2,] ♦

[1]*O.M. Beketov Kharkiv National University of Urban Economy, 17 Marshal Bazhanov Ave., Kharkiv 61002, Ukraine*

[2]*S. Kuznets Kharkiv National University of Economics, 9A Nauka Ave., Kharkiv 61166, Ukraine*

♦Address all correspondence to: A.M. Gokov, E-mail: 19amg55@gmail.com

The principle of construction of information devices of management of objects with intermittent mode of motion in the precise positioning zone on the basis of magnetometric converters is analyzed. Development of a device for stopping the movable object with the use of telecommunication data transmission, with increased accuracy and extended control range is suggested. The analytical expressions of the external field strength of the rod permanent magnet, which is used in the magneometric converter as a source of the information magnetic field, are obtained.

KEY WORDS: *movable object, telecommunication data transmission, magnetometer converter, permanent magnet, orthogonal component of magnetic field tension*

1. INTRODUCTION

For effective positioning of objects with a discontinuous mode of the movement such as elevators, cable cars, unmanned vehicles, modular mobile systems, cranes, stacker cranes, conveyors, gantry robots, mobile manipulators, ecological equipment components, it is necessary to ensure their precision control systems. The development of appropriate devices to develop reliable information on the location of the movable object in the zone of exact stopping in the specified place is relevant. The primary information devices are usually a range of sensors of different principles of operation: mechanical, eddy current, ultrasonic, magnetic, laser and the like.

In the device of movement control, in particular, for their exact stopping, it is also advisable to use magnemetric converters, which are a combination of magnetic tags recorded on a steel structure, or permanent magnets with magneto-sensitive elements (current-sensitive magnetic reading heads, Hall sensors, reed switches, magnetoresistive bridges, ferroprobes bridges, ferro-probe). In the development of precise stop moving units significant effect gives the use of the appropriate orthogonal component of the outer field recorded on the ferromagnetic guide of the magnetic label or permanent magnet.

Typically, such areas with a high steepness of the change of the field intensity and a wide control range in the vicinity of the exact stopping point are created by bar magnets arranged with a magnetic axis along the movement of the object.

There are a known information devices that are useful for creating traffic control systems. In [1] to combat the unwanted fluctuations in the bridge systems during displacement and especially in the endpoint of transportation, a reliable controller is applied. To achieve minor angles of swing and also to account for potential error of the system, a controller is chosen, which combines the approach of linearization of feedback and control of time delay. It is a delay control that is used to stabilize the feedback for a nonlinear system under the influence of uncertainty. However, the system does not provide sufficient positioning accuracy for the overhead crane.

In [2] a method is described for the exact stop of the lift car floor at the level of the landing site. It consists in the fact that the lift control system generates commands sent to the actuator, which is the winch brake, using signals from the sensors in the shaft to regulate the elevator control object. Further, the system, using a measuring element, fixes the position of the elevator car and, based on the measurement results, generates a command to ensure the influence of the executive mechanism on the object of regulation. The method improves the accuracy of stopping the cab relative to the landing site. The disadvantage of this method is its insufficient performance.

In [3] it is noted that the shunts of the sensor of the exact stop of the elevator car are installed at such a distance that the difference between the levels of the car floor and the surface was the same when stopping the loaded and empty car when it moves in one direction. It is accepted to estimate accuracy of a stop by size of a half-difference of brake ways of a cabin at movement in one direction with cargo and emptiness: at movement downwards $\Delta = \pm (hl - he)/2$, at movement upwards $\Delta = \pm (he - hl)/2$, where he, hl is the braking distance of the empty and loaded cab, respectively. The disadvantage of this assessment of the accuracy of stopping the car is that it does not take into account the intermediate load of the elevator car. In accordance with the instructions adopted, cabin stop accuracy should be kept in limits that do not exceed: For hospital lifts and freight elevators with monorail ±15 mm, for others – ±50 mm.

When using a controlled three-phase AC drive and a DC drive, high stopping accuracy can be achieved. A significant increase in the positioning accuracy of a moving object, including an elevator, provides the use of magnetometric transducers, the center of the source of the magnetic field which is rigidly attached to the stopping point. For example, the device for locating the magnetic tag center [4] which is applied to the guide rail structure along the motion of the vehicle, comprises a double-shaft flow-sensitive magnetic read head, the signal winding of which is connected to the indicator through a serially connected first phase detector, a first threshold element and the logic element AND. The excitation winding is connected to the exciter. The measuring winding is coupled to the second input of the logic element AND through a serially coupled amplitude detector, the second threshold element and circuit NO. It also contains a trigger, the outputs of which are connected with the additional inputs of the indicator, and the inputs are connected to the outputs of the third and fourth threshold elements, the inputs of which are connected to the output of the second phase detector. The inputs of phase detector are connected to the measuring winding. The device provides an exact stop signal with an indicating the direction of movement of the transport object. The disadvantage of this device is that it does not have a signal for switching cruising speed to a lower one, which may cause a "run" of a transport unit through a zone of exact stop.

In order to improve the accuracy and stability of the devices being developed, instead of rectangular control signals that form the movement of the transport unit directly near the narrow precision stop zone, it is proposed to generate control signals that, when the vehicle is brought closer to the zone of exact stop, decreases by almost to zero [5]. In a device for stopping a moving object [6], which contains three digital non-polar Hall sensors, the second and third of which are located opposite the other, and the first is perpendicular to them. The outputs of three unipolar digital Hall sensors are connected to an electronic circuit, which consists of the appropriate combinations of elements NOT and AND connected to the inputs of the microprocessor device. This design and principle of operation of the device provide a higher resolution, accuracy and level of element base unification.

Our paper presents a the development of information control devices for stopping moving objects based on magnetometric converters with the use of telecommunication data transmission with increased accuracy and an extended control range is proposed.

2. THE PROPOSED DEVICE FOR PRECISE POSITIONING OF THE MOVABLE OBJECT

We have proposed a device for precise positioning of a moving object, in which the magnetometric transducer is used, based on a rod rectangular permanent magnet, the magnetic axis of which is directed along the motion, and five unipolar digital Hall sensors. The essence of the new technical solution is explained by the drawing (Fig. 1), which depicts a device containing:

- The first (1), second (2), and third (3) unipolar digital sensors Hall, the second (2) and (3) of which are located in the same plane with opposite polarity, and the first one – between them and perpendicular to them;
- Elements NOT of (4-8); elements AND (9-14);

– A pivot permanent magnet (15) located by the magnetic axis along the course of the moving object (not shown in the drawing);
– Microprocessor device (16);
– Fourth (17) and fifth unipolar digital Hall sensors, located from the first (1) unitary of a unipolar digital Hall sensor in opposite directions in one plane with opposite polarity at a distance equal to the length of l pivot constant magnet (15);
– Additional elements NOT (19), (20); elements OR (21), (22); signal transmitter (23); transmitting antenna (24); receiving antenna (25); receiver signals (26); converting-intensifying channel (27) and executive mechanism (28).

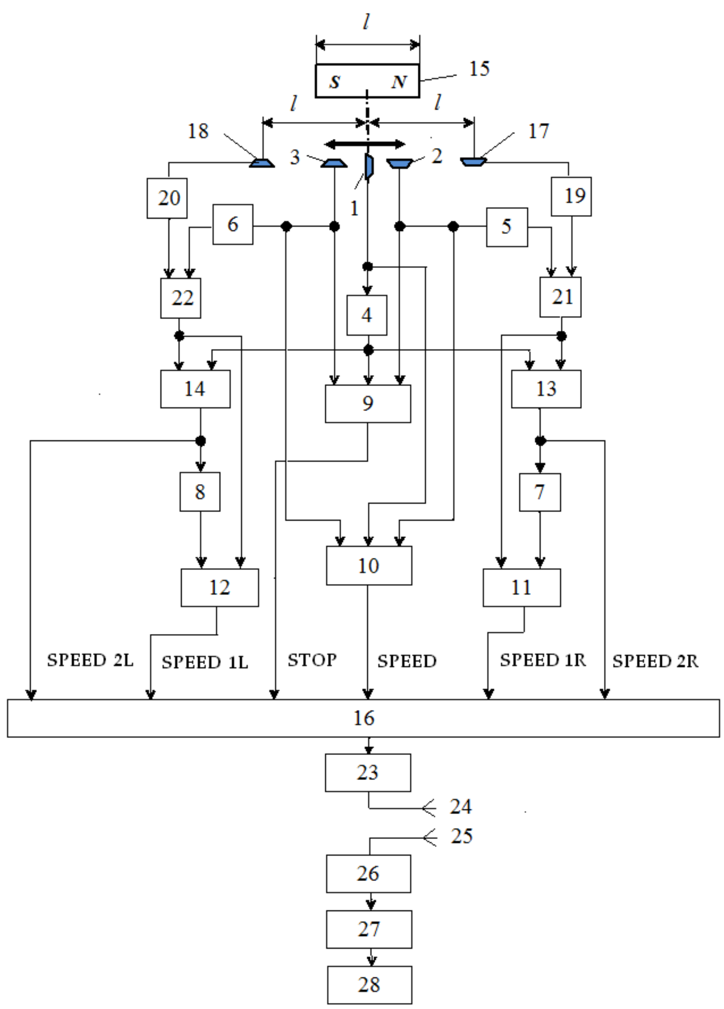

FIG. 1: Block diagram of the device for precise positioning of a moving object

Figure 2 shows diagram operation of the proposed device.

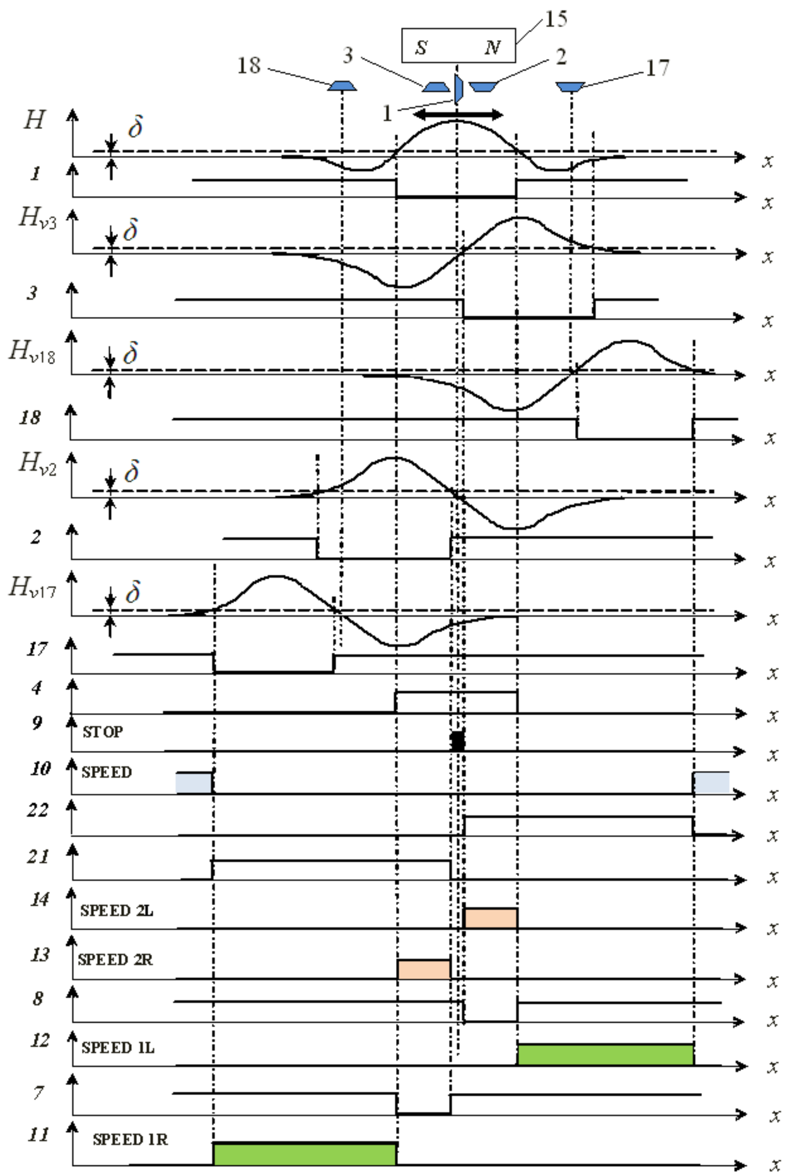

FIG. 2: The block diagram operation of the proposed device

The device works as follows. Preliminarily, a magnetic mark is applied to the steel guide structure with a magnetic head for longitudinal recording. A rod permanent magnet (15), attached at a designated place of precise positioning of a moving object (shown in Figs. 1 and 2), can also be used. The first (1) unipolar digital Hall sensor responds to the horizontal component of the field strength H_h of the rod permanent magnet (15) (diagram H_h, Fig. 2), the second (2), third (3), fourth (17) and fifth (18) unipolar digital Hall sensors respond to the vertical component of the field strength of the rod permanent magnet (15) (diagrams H_{v2}, H_{v3}, H_{v17}, H_{v18}, Fig. 2). When a controlled movable object moves, on which unipolar digital Hall sensors (1-3), (17), (18) are located, the first 1 digital Hall sensor is triggered when the signal H_h exceeds the threshold Δ (diagram 1, Fig. 2), the second (2), the third (3), the fourth (17) and the fifth (18) the unipolar digital Hall sensors are triggered when $H_v > \delta$ (diagrams 2, 3, 17, 18, Fig. 2)

When moving the movable object with cruising speed on the output of the element AND (10) generates signal SPEED (diagram 10, Fig. 2).

When moving the controlled object in the direction of "Right" at the time of operation of the fourth (17) unipolar digital Hall sensor (diagram 17, Fig. 2) include the elements NOT (19), element OR (21) (diagram 21, Fig. 2) and element AND (11). On the output of element OR (21) produced a signal SPEED 1R (diagram 11, Fig. 2), which translates the movement of a moving units from cruising speed to reduced.

With further movement "Right", the second unipolar digital Hall sensor 2 is triggered (diagram 2, Fig. 2), the element NOT (5) is turned on. Element OR (21) (diagram 21 in Fig. 2) together with element AND (11) continue to produce the SPEED 1R signal (diagram 11, Fig. 2).

As the object "Right" continues to move the first (1) unipolar digital Hall sensor (plot 1, Fig. 2), element NOT (4) (plot 4, Fig. 2), and element AND (13) are triggered. This leads to the generation of signal SPEED 2R (plot 13 in Fig. 2). This signal converts the movement of the controlled unit to a "creeping" speed and ensures its smooth stop and through the element NOT 7 (plot 7, Fig. 2) stops generating the signal SPEED 1R (plot 11 of Fig. 2).

At the moment of coincidence of the center of the first (1) unipolar digital sensor Hall with the center of the rod permanent magnet (15) at the output of the element AND (9), a signal of an exact stop STOP in the narrow zone is generated (diagram 9, Fig. 2).

When the controlled object moves in the direction of the "Left" the device works similarly.

The control signals are fed to the inputs of the microprocessor device (16), which, after processing in it through the signal transmitter (23), are fed to the transmitting antenna (24). Further, the signals are received by the receiving antenna (25) and through the signal receiver (26) and the converting-amplifying channel (27) are fed to the executive mechanism (28).

The proposed device by increasing the range of the smooth braking of the moving object will improve the reliability of the device and enhance its functionality.

3. MATHEMATICAL MODEL FOR CALCULATING THE FIELD OF A ROD PERMANENT MAGNETS

Analytical studies of the permanent magnets field configuration are a complex problem, which in the general case is the three-dimensional static scattering field and theoretically cannot be solved. But for magnetic systems, where magnets have a fairly simple shape (parallelepiped, ring, cylinder), there are many analytical approaches that are practiced by different authors to calculate the fields of such magnets. Thus, in [7,8], the analytical calculation of the field created by permanent magnetic rings is presented. For an axial ring magnet using the Coulomb approach, radial and axial components are deduced. In [9] analytical expressions of the magnetic induction of a field of cylindrical permanent magnets are presented.

Now a large number of effective machine methods for calculating the fields of complex magnetic systems have been developed and used, taking into account the nonlinear dependence of magnetic penetration on the field strength. In [10], the basic formulas for the finite element method of three-dimensional static potential magnetic fields are derived in the regions filled with non-linear nonhysteresis anisotropic media. Work [11] is devoted to the calculation of the magnetic field based on the ANSYS software package.

When analyzing the distribution of the magnetic field, which is created by a permanent magnet of a magnetometric transducer, subject to the introduction of certain assumptions, the main of which are the constructive idealization of the magnet body and its isotropy, it is possible to consider a two-dimensional potential problem, which is described by differential equations of elliptical type. The solution of such problems takes place only in some cases and is a relatively simple, but acceptable and universal expression for analysis.

In order to analytically determine the area of spatial change of the field, consider an idealized two-dimensional model of a rod rectangular magnet in the presence of a near-side edge of a point-sensitive magnetic element (MSE) (flux-sensitive magnetic head, Hall sensor or ferro probe), which does not distort the field picture. In the study of the external field of the magnet used the method of analysis of static fields, given in [12,13]. The essence of the method is to represent the body of a magnet in the form of residual magnetization, its decomposition into a spatial spectrum and in solving the boundary value problem for one arbitrary harmonic component with subsequent integration over all components of the spectrum, determining the scalar magnetic potential caused by all harmonics of the spectrum, and finding the orthogonal components of the external field strength of the magnet.

The field analysis is carried out for a rectangular rod with length 2Δ and thickness a. In addition, with high accuracy for practice, the relative magnetic penetration μ of a magnet can be considered as a constant value, and MSE as a point. Idealized two-dimensional model of the rod magnet is shown on Fig. 3.

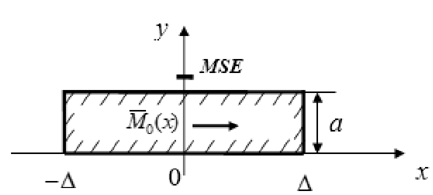

FIG. 3: An idealized two-dimensional model of a rod magnet

The residual magnetization of the adopted model of the rod magnet can be determined by expression:

$$\overline{M}_0(x) = \bar{i} M_{0m} p_\Delta(x), \tag{1}$$

where M_{0m} is the amplitude value of residual magnetization; $\bar{i}$ is the single vector that coincides in the direction with the x axis; $p_\Delta(x) = 1$ for $|x| \le \Delta$ and $p_\Delta(x) = 0$ for $|x| > \Delta$.

Figure 4 shows the distribution of magnetization along the x axis.

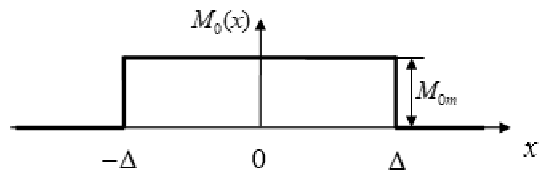

FIG. 4: The distributions of magnetization along the *x* axis

For the excepted model we can find the spatial spectrum of magnetization.

The decomposition of $\overline{M}_0(x)$ in the Fourier integral is written in the form:

$$\overline{M}_0(x) = {}^{3}M_{0m} \frac{2}{\pi} \int_0^\infty \frac{\sin \Delta\omega}{\omega} \cos x\omega d\omega. \tag{2}$$

For an arbitrary harmonic component of the spatial spectrum of frequency $\omega = \Omega \neq 0$ we can write:

$$\overline{M}_{0\Omega} = {}^{3}M_{m\Omega} \cos \Omega x, \tag{3}$$

where $M_{m\Omega} = \frac{2}{\pi} M_{0m} \frac{\sin \Delta\Omega}{\Omega}$ is the amplitude of the magnetization of the frequency harmonic Ω, for which the boundary value problem is solved (Fig. 5).

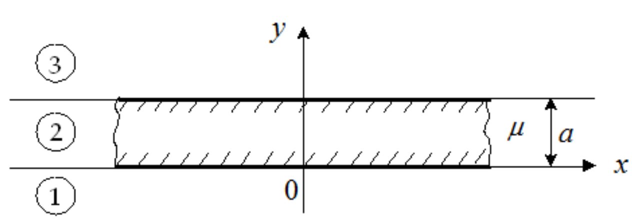

FIG. 5: Model of the harmonic component of an arbitrary frequency of magnetization

The equation relatively to the scalar potential of the magnetic field has the form:

$$\Delta\varphi_i = \frac{div\bar{M}_{0\Omega}}{\mu} = -\frac{\Omega M_{m\Omega}\sin\Omega x}{\mu}, з = 2; \ \ \Delta\varphi_i = 0, з = 1.3. \quad (4)$$

where Δ is the Laplace operator.

The solution of the differential Eq. (4) can be found as:

$$\begin{aligned} \varphi_1 &= \grave{A}_1 \mathring{a}^{\Omega y} \sin\Omega x, \\ \varphi_2 &= (A_2 \mathring{a}^{\Omega y} + B_2 e^{-\Omega y})\sin\Omega x + Q(x), \\ \varphi_3 &= \grave{A}_3 \mathring{a}^{-\Omega y} \cos\Omega x \ , \end{aligned} \quad (5)$$

where $Q(x) = \frac{M_{0\Omega}}{\mu\Omega}\sin\Omega x$ is the partial solution of the Poisson equation for area 2.

On each of the two boundaries, the following boundary conditions are perform:

$$\phi_з = \phi_{з+1} \ ; \ \ \mu_з \frac{\partial\phi_з}{\partial y} = \mu_{з+1}\frac{\partial\phi_{з+1}}{\partial y}. \quad (6)$$

Expressions for constant integration are found after substitution (6) in (4). The constant integration for the area of interest (where the magnetosensitive element is located) is equal to:

$$A_3 = -\frac{2M_{0\Omega}}{\Omega}\frac{1}{(\mu+1)^2\left[1-\left(\frac{\mu-1}{\mu+1}\right)^2 e^{-2\grave{a}\Omega}\right]}\left(1-\frac{\mu+1}{2}e^{\grave{a}\Omega}+\frac{\mu-1}{2}e^{-\grave{a}\Omega}\right). \quad (7)$$

Expression (7) can be transformed using the algebraic relation: $\frac{1}{1-z} = \sum_{\alpha=0}^{\infty} z^{\alpha}$, where $z^2 < 1$. Then we get:

$$A_3 = -\frac{2M_{0\Omega}}{\Omega}\frac{1}{(\mu+1)^2}\left(1-\frac{\mu+1}{2}e^{a\Omega}+\frac{\mu-1}{2}e^{-a\Omega}\right)\cdot\sum_{\alpha=0}^{\infty}\left(\frac{\mu-1}{\mu+1}\right)^2 e^{-2\alpha\Omega\alpha}. \quad (8)$$

After substituting (8) in (5) we find the scalar potential of the magnetic field in the region 3 which corresponds to the harmonic of the frequency Ω = *ω*. The potential caused by all components of the initial magnetization spectrum is determined in accordance with the expression (here the notation is introduced $m=\left(\frac{\mu-1}{\mu+1}\right)^2$):

$$\varphi_3=\frac{4}{\pi}\frac{M_{0m}}{(\mu+1)^2}\left[\int_0^\infty\frac{\sin\Delta\omega}{\omega}\sum_{\alpha=0}^{\infty}m^\alpha e^{-(y+2a\alpha)\omega}\frac{\cos x\omega}{\omega}d\omega-\right.$$
$$-\frac{\mu+1}{2}\int_0^\infty\frac{\sin\Delta\omega}{\omega}\sum_{\alpha=0}^{\infty}m^\alpha e^{-(y+2a\alpha-a)\omega}\frac{\cos x\omega}{\omega}d\omega+ \tag{9}$$
$$\left.+\frac{\mu-1}{2}\int_0^\infty\frac{\sin\Delta\omega}{\omega}\sum_{\alpha=1}^{\infty}m^\alpha e^{-(y+2a\alpha+a)\omega}\frac{\cos x\omega}{\omega}d\omega\right],$$

Reducing the integrals to tabular and taking into account the relation $\bar{H}=-\text{grad}\,\phi$, we obtain the expressions of the horizontal and vertical components of the field strength near the side of the permanent magnet:

$$H_{x3}=\frac{2}{\pi}\frac{M_{0m}}{(\mu+1)^2}\left[\sum_{\alpha=0}^{\infty}m^\alpha\left(\text{arctg}\frac{x+\Delta}{y+2a\alpha}-\text{arctg}\frac{x-\Delta}{y+2a\alpha}\right)-\right.$$
$$-\frac{\mu+1}{2}\sum_{\alpha=0}^{\infty}m^\alpha\left(\text{arctg}\frac{x+\Delta}{y+2a\alpha-a}-\text{arctg}\frac{x-\Delta}{y+2a\alpha-a}\right)+ \tag{10}$$
$$\left.+\frac{\mu-1}{2}\sum_{\alpha=0}^{\infty}m^\alpha\left(\text{arctg}\frac{x+\Delta}{y+2a\alpha+a}-\text{arctg}\frac{x-\Delta}{y+2a\alpha+a}\right)\right],$$

$$H_{y3}=\frac{1}{\pi}\frac{M_{0m}}{(\mu+1)^2}\left[\sum_{\alpha=0}^{\infty}m^\alpha\ln\frac{(y+2a\alpha)^2+(x-\Delta)^2}{(y+2a\alpha)^2+(x+\Delta)^2}-\right.$$
$$-\frac{\mu+1}{2}\sum_{\alpha=0}^{\infty}m^\alpha\ln\frac{(y+2a\alpha-a)^2+(x-\Delta)^2}{(y+2a\alpha-a)^2+(x+\Delta)^2}+ \tag{11}$$
$$\left.+\frac{\mu-1}{2}\sum_{\alpha=0}^{\infty}m^\alpha\ln\frac{(y+2a\alpha+a)^2+(x-\Delta)^2}{(y+2a\alpha+a)^2+(x+\Delta)^2}\right].$$

The values of H_{x3} and H_{y3} was calculated according to (10, 11) with the following parameters: $\mu = 100$, $a = 0.5\Delta$, $M_{0m} = 10^4$ A/m. Curve dependences H_{x3} and H_{y3} for the case of $y = 0.55\Delta$ are shown in Fig. 6.

Experimental verification of the configuration of the magnetic field calculated according to the expressions (11, 12) was performed on a rectangular permanent magnet with dimensions: length $2\Delta = 39$ mm, thickness a = 9.5 mm (a = 0.5Δ), width 24 mm. As can be seen from Fig. 6, the theoretical and experimental orthogonal components of the magnet magnetic field intensity practically coincide.

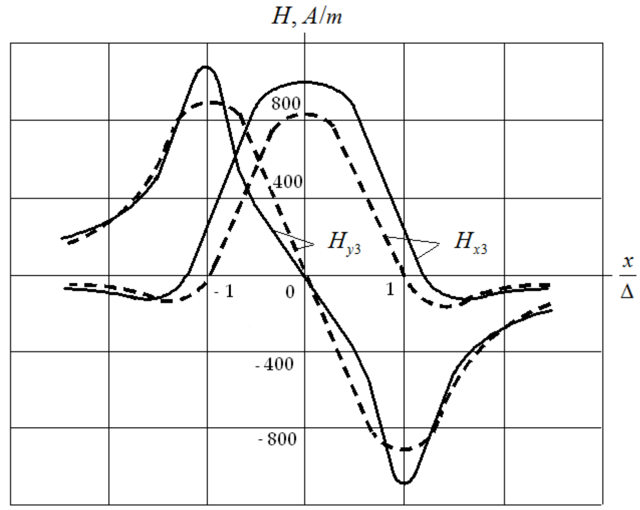

FIG. 6: Theoretical (solid line) and experimental (dashed line) dependencies of the H_{x3} and H_{y3} components of the orthogonal components of the external field strength for a rectangular rod for case $y = 0.55\Delta$

Some discrepancy between them is explained, firstly, by the fact that the width of the magnet in the idealized model was considered infinite, and in a real magnet it is equal to only 2.55 a, secondly, the lines of tensions extend from the entire surface of the real magnet, and from the two-dimensional idealized model rod magnet - only from the poles. This explains the more sharp peaks of the theoretical bi-pulse curve of the intensity H_{y3} of the above model over its poles. However, some difference between theoretical and experimental data does not significantly affect the accuracy of magnetometric transducers, as the appropriate choice of the gap between the surface of the permanent magnet and the magnetically sensitive elements achieves acceptable sensitivity and accuracy of the device.

Similar dependencies serve as a source of information in the development of control systems for precise stopping of widely used moving objects based on magnetometric transducers.

4. CONCLUSIONS

An overview of known mobile device management devices has shown that in order to increase their accuracy, resolution and expansion of the application perspective is development of precise positioning devices, in which magnemetric converters are used, which are a combination of magnetic tags, recorded on a directing steel structure, or permanent magnets with magneto-sensitive elements (threaded by magnetic reading heads, sensors Hall, ferro-probe, reed switches, magnetoresistors).

It is proposed the information device for stopping the movable object in order to increase the accuracy and control range of the precise positioning zone is applied by the metrological converter, which comprises the original scheme of five unipolar digital Hall sensors. It can serve as an example of developing similar devices.

The new analytical expressions for horizontal and vertical components of the outer field of a permanent bar rectangular magnet that are located on the magnetic axis along the direction of the moving object are obtained. These components in the control systems of mobile units with a discontinuous nature of the movement represent the basis for the location of magneto-sensitive elements near the surface of the information magnetic field sources in the most rational manner.

REFERENCES

1. Cheng, C.C. and Chen, C.Y., (1996) Controller design for an overhead crane system with uncertainty, *Control Engineering Practice*, **4** (5), pp. 645-653.
2. Lavrov, V.V. (2005) *The way to accurately stop the floor of the elevator cabin at the level of the landing site*, Patent RF No 2202508, 5 p, (in Russian).
3. Volkov, D.P., (1999) *Lifts*, Russia: ABU Publ., 480 p., (in Russian).
4. Mogila, V.I., Gorbunov, M.I., and Smyrnyi, M.F., (2016) *Device for finding the center of a magnetic tagm*, Patent Ukraine No 108490, 5 p, (in Ukrainian).
5. Smyrnyi, M.F. and Ivanjva, O.R., (2020) *Device for stopping the vehicle*, Patent Ukraine No 120797, 5 p, (in Ukrainian).
6. Smyrnyi, M.F. and Polivianchuk, A.P., (2020) Magnemetric converters of information devices of control of mobile objects, *Technical Electrodynamics*, **2**, pp. 10-16, (in Ukrainian).
7. Babic, S., (2008) Improvement in the analytical calculation of the magnetic field produced by permanent magnet rings, *Progress in Electromagnetics Research C*, **5**(1), pp. 71-82.
8. Ravaud, R., Lemarquand, G., Lemarquand, V., and Depollier, C., (2008) Analytical Calculation of the Magnetic Field Created by Permanent-Magnet Rings, *IEEE Transactions on Magnetic*, **44**(8), pp. 271-282.
9. Ravaud, R., Lemarquant, G., Babic, S., Lemarquand, V., and Akyel, C., (2010) Cylindrical magnets and coils: fields, forces, and inductances, *IEEE Transactions on Magnetic*, **46**(9), pp. 372-382.
10. Karashetsky, V.P., (2013) Calculation of three-dimensional potential magnetic fields by the finite element method, *Scientific Bulletin of NLTU of Ukraine*, **23.12**, pp. 379-381, (in Ukrainian).
11. Bilyi, P.M. and Oprichko, V.V., (2007) Calculation of the magnetic field based on the ANSYS software package, *Bulletin of the KPUU*, **1**(42), pp. 42-44.
12. Laufer, M.S. and Chatskis, L.H., (1973) Analysis of fields of magnetic heads, *Electrical Engineering*, **10**, pp. 1059-1062.
13. Chatskis, L.H., (1973) Study of static fields, *Electricity*, **1**(2), pp. 47-50.